Available online at www.sciencedirect.com
ScienceDirect
Journal of Electrostatics 65 (2007) 728–734
Journal of ELECTROSTATICS
www.elsevier.com/locate/elstat

EHD flow measured by 3D PIV in a narrow electrostatic precipitator with longitudinal-to-flow wire electrode and smooth or flocking grounded plane electrode

A. Niewulis[a], J. Podliński[a,*], M. Kocik[a], R. Barbucha[a], J. Mizeraczyk[a,b], A. Mizuno[c]

[a]*Centre for Plasma and Laser Engineering, The Szewalski Institute of Fluid Flow Machinery, Polish Academy of Sciences, Fiszera 14, 80-952 Gdańsk, Poland*
[b]*Department of Marine Electronics, Gdynia Maritime University, Morska 81-87, 81-225 Gdynia, Poland*
[c]*Department Ecological Engineering, Toyohashi University of Technology Tempaku-cho, 441-8580 Toyohashi, Japan*

Received 5 April 2007; received in revised form 9 May 2007; accepted 17 May 2007
Available online 21 June 2007

Abstract

In this work, results of three-dimensional (3D) Particle Image Velocimetry (PIV) measurements of the electrohydrodynamic (EHD) flow velocity fields in a narrow electrostatic precipitator (ESP) with a longitudinal-to-flow placed wire electrode are presented. The ESP was a narrow transparent acrylic box (90 mm × 30 mm × 30 mm). The electrode set consisted of a single wire discharge electrode and two plane collecting electrodes. Either two smooth stainless-steel plates or two stainless-steel plane meshes with nylon flocks were used as the collecting electrodes. The 3D PIV measurements were carried out in two parallel planes, placed longitudinally to the flow duct. The positive DC voltage of up to 9.5 kV was applied to the wire electrode through a 10 MΩ resistor. The collecting electrodes were grounded. The measurements were carried out at a primary flow velocity of 0.5 m/s. Obtained results show that the flow patterns for the smooth-plate electrodes and for the flocking plane electrodes are similar in the bulk of the flow. However, the flow velocities near the flocking plane electrodes are much lower than those near the smooth-plate electrodes. This is a beneficial phenomenon, because the lower the flow near the collecting electrodes, the lower re-entrainment of the particles deposited on the collecting electrodes occurs.

Keywords: Narrow electrostatic precipitator; EHD flow; 3D PIV; Flow measurement; Flocking electrode

1. Introduction

Many research studies aimed at improving the collection efficiency of fine particles in conventional electrostatic precipitators (ESPs) have been carried out for the past years [1–12]. Collecting of fine particles is of crucial importance, because many of them, in the size range 0.1–1 μm have a detrimental effect on both human and animal health. The fine particles may contain hazardous trace elements such as lead, mercury, arsenic, zinc, biological agents and others.

Investigations of the particle collection phenomenon showed that the fine particle collection efficiency in typical ESPs with smooth-plate collecting electrodes is low (70–80%) [2]. However, it was also shown that the use of flocking plane electrodes as the collecting electrodes increased the collection efficiency of fine particles up to 94% [3]. In [3], the flocking plane electrodes were manufactured by depositing dielectric nylon fibers on a metal wire mesh. The fibers had the form of cylindrical granules of a diameter of 19.5 μm and a height of 1 mm.

The movement and precipitation of particles in the ESPs depend mainly on the electric field, space charge, gas flow velocity, particle physical parameters, electrode geometry and the electrohydrodynamic (EHD) secondary flow. The interaction between these factors results in considerable turbulences of the flow between discharge and collecting electrodes [4–10]. Atten et al. [11] and Yamamoto [12] suggested that the flow turbulences in ESPs lower the fine particle collection efficiency. Therefore, the turbulence should be reduced to improve the performance of ESPs. Improving other factors, like ESP electrode geometry or ESP operating conditions may also increase the fine

*Corresponding author.
E-mail address: janusz@imp.gda.pl (J. Podliński).

0304-3886/$ - see front matter © 2007 Elsevier B.V. All rights reserved.
doi:10.1016/j.elstat.2007.05.006

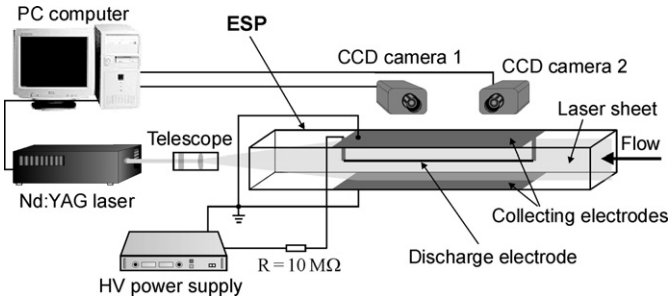

Fig. 1. Experimental set-up.

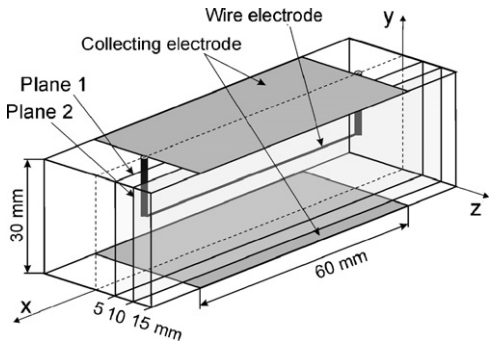

Fig. 2. ESP with observation planes marked: Plane 1 ($z = 5$ mm), Plane 2 ($z = 10$ mm).

particle collection efficiency. Replacement of the typical smooth-plate collecting electrodes by the flocking plane electrodes was suggested as a means of improving the fine particle collection efficiency [3,13].

In this paper, the performance of a narrow ESP, having a wire discharge electrode, placed along the flow duct, and two sets of plane collecting electrodes (Figs. 1 and 2), was studied. In typical ESP, the wire discharge electrode (or electrodes) is placed transversely to the flow. The first plane electrode set consisted of two smooth plates (called the smooth-plate collecting electrodes). The second set was formed by two stainless-steel plane meshes covered with nylon flocks (called the flocking plane collecting electrodes). Such an ESP electrode geometry is called a longitudinal wire-plane electrode arrangement. Our investigations focused on measuring the flow patterns in the longitudinal-type ESP. For that we used the three-dimensional (3D) Particle Image Velocity (PIV) [14,15] with either the smooth-plate or flocking plane electrodes. To our knowledge, the flow patterns in such an ESP have not been measured yet.

The measurements were carried out for the positive voltage polarity of the wire discharge electrode in two measurement planes, placed along the flow duct. Due to the limited size of this paper only results for one plane are presented.

2. Experimental apparatus

The experimental apparatus used in the present investigations consisted of an ESP, high-voltage power supply and 3D PIV equipment for the measurement of velocity field (Nd:YAG laser, cylindrical telescope, two CCD cameras and PC computer)—Fig. 1.

The ESP was a narrow transparent acrylic box, 90 mm long, 30 mm wide and 30 mm high (Figs. 1 and 2). The electrode set was formed by a single wire discharge electrode and two plane collecting electrodes. The stainless-steel wire discharge electrode (diameter of 0.1 mm, length of 60 mm) was mounted in the middle of the ESP, along with the flow direction (Figs. 1 and 2). The collecting electrodes (60 mm long and 30 mm wide) were placed on the top and the bottom of the ESP. Two kinds of the plane collecting electrodes were used: the first consisted of two smooth plates (the smooth-plate collecting electrodes) and the second was formed by two stainless-steel plane meshes covered with nylon flocks (the flocking plane collecting electrodes). The flocking plane electrodes were as in [3].

Positive voltage up to 9.5 kV was supplied to the wire electrode through a 10 MΩ resistor. Air flow seeded with cigarette smoke was blown along the ESP duct with an average velocity of about 0.5 m/s. The cigarette smoke was used for visualization of the flow.

The 3D PIV measurements of the flow velocity field were carried out in two parallel planes defined by a laser sheet of a thickness of 1 mm, formed from the Nd:YAG laser beam by the cylindrical telescope. Both measurement planes were placed along the flow direction, perpendicular to the collecting electrodes. The distance of the laser sheet from the wire electrode was either 5 mm (Plane 1) or 10 mm (Plane 2) (Fig. 2). As mentioned, in this paper only results for plane 1 are presented, because of the limited size of this paper.

Two CCD cameras, connected to the PIV computer, were focused on the observation area at different angles, as shown in Fig. 1. This enabled us (after the calibration process) to get all three components of the velocity in the measured planes.

All velocity fields presented in this paper were obtained by averaging the results of 100 PIV measurements. This means that every velocity field presented was time-averaged. Based on the measured velocity fields, the corresponding flow streamlines were calculated.

3. Results

The results of the 3D PIV measurements for both electrode arrangements (the wire-smooth-plate and the wire-flocking plane) in plane 1 are shown in Figs. 3–9. They present the flow patterns (velocity fields and corresponding flow streamlines) in the x–y plane as well as the x-, y- and z-component of the flow velocity. The x-component of velocity is parallel to the flow duct, while the y- and z-components have the transverse direction to the flow duct. The primary flow average velocity was 0.5 m/s. At this velocity, the Reynolds number was $Re = 955$. It was

calculated using the formula [16]:

$$\mathrm{Re} = V \times L/v. \quad (1)$$

The parameters used were: $V = 0.5\,\mathrm{m/s}$ (the primary flow velocity), $L = 0.03\,\mathrm{m}$ (the distance between the collecting electrodes) and $v = 1.57 \times 10^{-5}\,\mathrm{m^2/s}$ (the air kinematic viscosity).

The flow patterns in plane 1 for the wire-smooth-plate electrode arrangement, when no voltage was applied, are presented in Figs. 3a–c. As it can be seen from these figures, the movement of the seed particles in the ESP is regular and directed in accordance with the primary flow direction. The velocity z-component is very low and reaches values lower than 0.1 m/s. Thus the flow is laminar. For the wire-flocking plane electrode arrangement, the flow velocity fields were very similar (not shown in this paper).

The results of 3D PIV measurements in plane 1 in the ESP with the wire-smooth-plate electrode arrangement for a positive voltage of 9.5 kV are presented in Figs. 4a and b. The average total discharge current was 49 μA. At this current, the EHD number, which is related to the electric forces was 1.9×10^7. The EHD number was calculated using the formula [16]:

$$\mathrm{Ehd} = I \times L^3/(v^2 \times \rho \times \mu_i \times A) \quad (2)$$

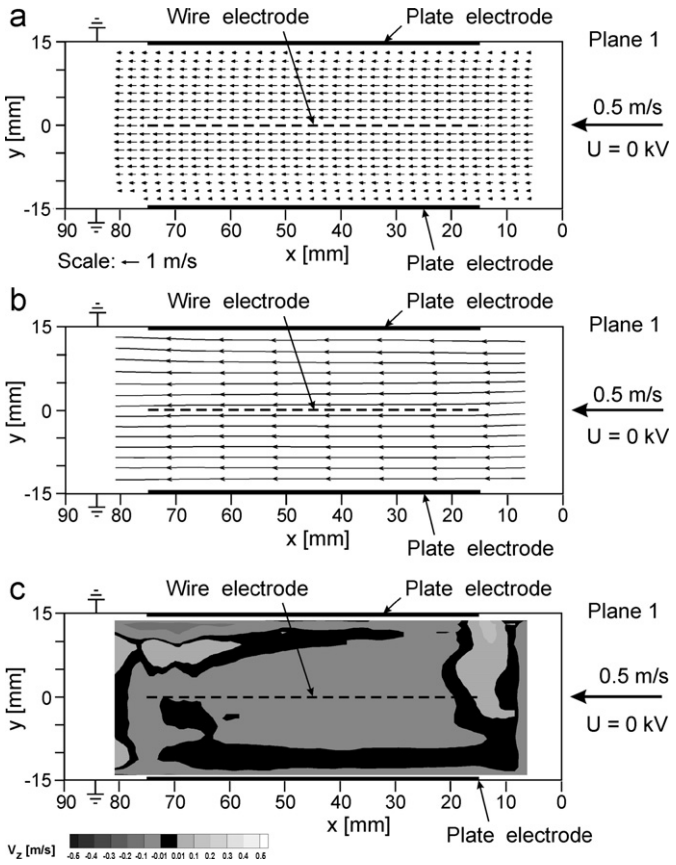

Fig. 3. Results of 3D PIV measurement in plane 1 (x–y plane) in the wire-smooth-plate ESP when no voltage was applied: (a) the flow velocity field, (b) corresponding flow streamlines and (c) the velocity z-component.

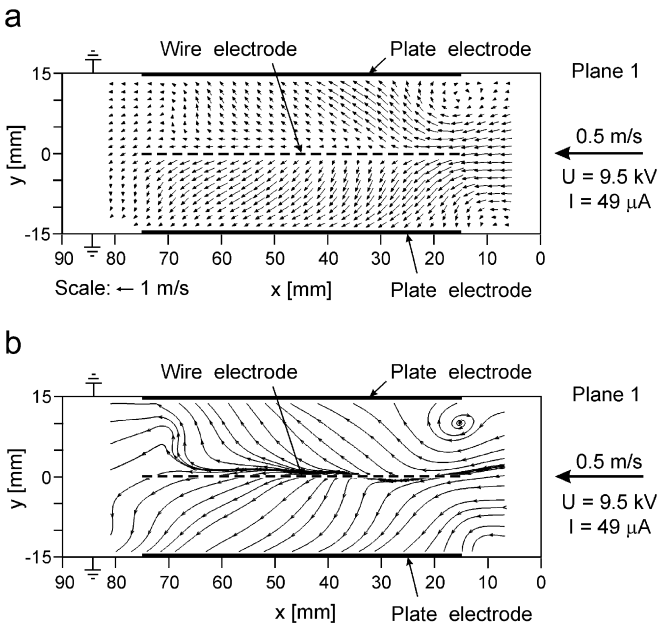

Fig. 4. Results of 3D PIV measurement in plane 1 (x–y plane) in the wire-smooth-plate ESP for positive voltage of 9.5 kV: (a) the flow velocity field and (b) corresponding flow streamlines. The average total discharge current 49 μA.

with the parameters as follows: $I = 49\,\mu\mathrm{A}$ (the average total discharge current), $L = 0.03\,\mathrm{m}$ (the distance between the collecting electrodes), $v = 1.57 \times 10^{-5}\,\mathrm{m^2/s}$ (the air kinematic viscosity), $\rho = 1.205\,\mathrm{kg/m^3}$ (the air density), $A = 0.0036\,\mathrm{m^2}$ (the discharge area equal to the doubled area of the collecting electrode) and $\mu_i = 6.46 \times 10^{-5}\,\mathrm{m^2/V\,s}$ (the ion mobility). The ratio of the EHD number to the Reynolds number squared was 21 ($\mathrm{Ehd/Re^2}$ describes the ratio of the electric forces to the inertial force).

Due to the voltage applied, the flow patterns shown in Figs. 4a and b changed significantly when compared to those shown in Figs. 3a–c (no voltage applied). It is seen from Figs. 4a and b that a secondary flow, caused by the EHD forces, is formed in the flow duct. The particle flow pattern in the x–y plane is affected by the electric field even before the discharge region, which begins at $x = 15\,\mathrm{mm}$. Starting from this point, the particle trajectories are strongly bent towards the plate electrodes. However, the most pronounced deflection of the particle trajectories towards the smooth-plate electrodes occurs at $x = 30$–$40\,\mathrm{mm}$. As seen from Figs. 4a and b, also a vortex occurs in the secondary flow, at $x = 10$–$20\,\mathrm{mm}$.

The results of 3D PIV measurement in plane 1 in the ESP with the wire-flocking plane electrode arrangement for a positive voltage of 9.4 kV are presented in Figs. 5a and b. The average total discharge current was 60 μA. At this current, the EHD number was 2.35×10^7, and the ratio $\mathrm{Ehd/Re^2}$ was 26.

Figs. 5a and b show similar effects, caused by the applied voltage, as in the wire-smooth-plate ESP (Figs. 4a and b): the particle trajectories are strongly bent towards the flocking plane electrodes, and two vortices are formed in

the secondary flow (the first at $x = 10$–20 mm and the second at $x = 65$–75 mm).

However, an important difference between the EHD flow in both electrode arrangements (the wire-smooth-plate and the wire-flocking plane) can easily be seen from Figs. 6a and b, which show the velocity x-component for the wire-smooth-plate ESP and the wire-flocking plane ESP at similar discharge parameters. The velocity x-component (i.e. directed parallel to the collecting electrodes) is for the wire-flocking plane ESP lower than that for the wire-smooth-plate ESP. This may suggest that the lower flow velocity near the collecting electrodes would cause lower re-entrainment of the particles deposited on the collecting electrodes in the practical ESPs.

The velocity y-component (i.e. directed towards collecting electrodes (Figs. 7a and b)) is similar for both electrode arrangements. The highest velocity values of the y-component reach 0.5 m/s.

Figs. 8 and 9 show the velocity z-component for the wire-smooth-plate and wire-flocking plane ESPs, respectively. As it can be seen from these figures, the properties of the particle flow in the z-direction are the same for both electrode arrangements. However, the particle movement in the z-direction is less regular as it was when no voltage was applied (Fig. 3c). When the voltage is applied, the particles in the central part of the ESP duct (i.e. at $x = 25$–80 mm, $y = -5$ to 5 mm) are moved towards the wire electrode. On the other hand, the particles near the collecting electrodes are pushed towards the side walls. In both cases, i.e., in the wire-smooth-plate and the wire-flocking plane ESPs, the values of the z-component velocity are relatively high, but in the wire-flocking plane ESP they are lower than those in the wire-smooth-plate ESP. The velocity z-component for the wire-flocking plane ESP reaches -0.3 m/s near the duct midline and $+0.3$ m/s at the flocking plane electrodes, when for the wire-smooth-plate ESP reaches -0.5 m/s near the duct midline and $+0.4$ m/s at the plate electrodes. Therefore, we may conclude that for both cases the EHD secondary flow is undoubtedly three dimensional.

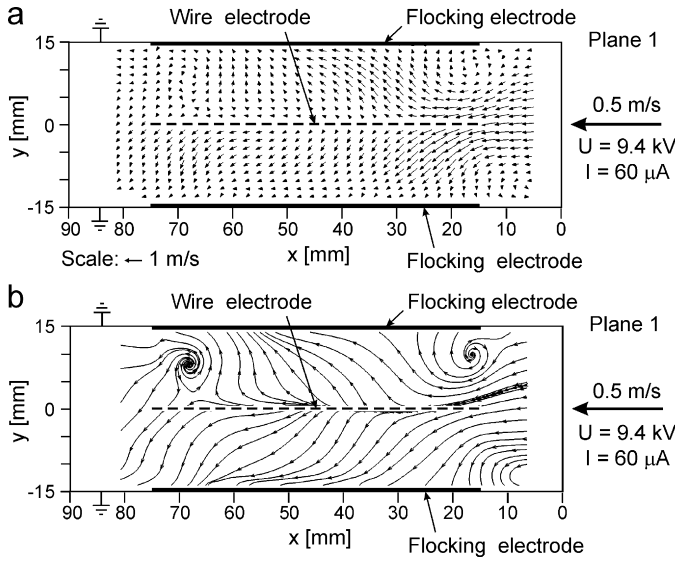

Fig. 5. Results of 3D PIV measurement in plane 1 (x–y plane) in the wire-flocking plane ESP for positive voltage of 9.4 kV: (a) the flow velocity field and (b) corresponding flow streamlines. The average total discharge current 60 μA.

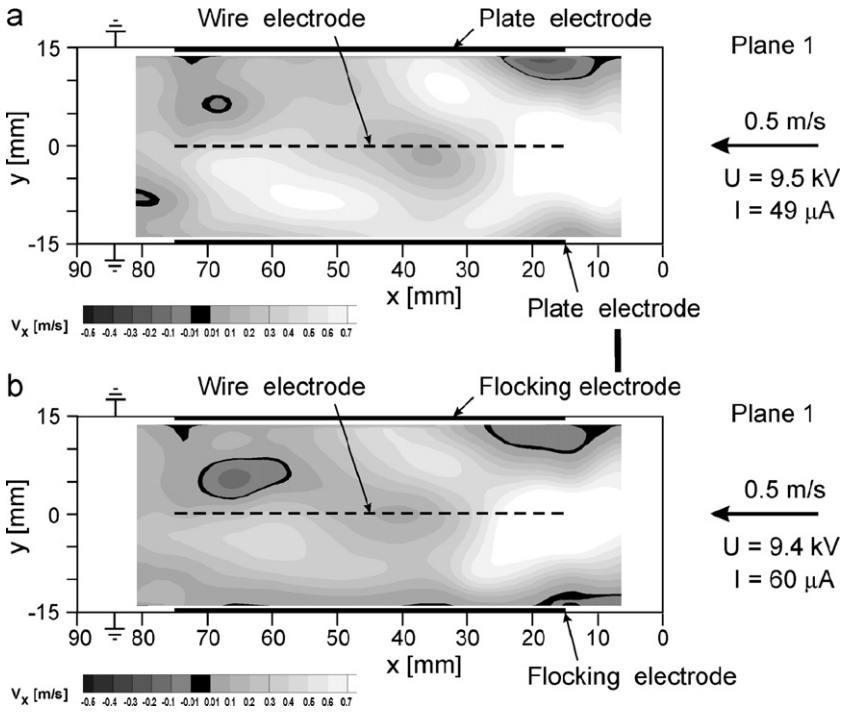

Fig. 6. Velocity x-component in plane 1: (a) in the wire-smooth-plate ESP for positive voltage of 9.5 kV and (b) in the wire-flocking plane ESP for positive voltage of 9.4 kV.

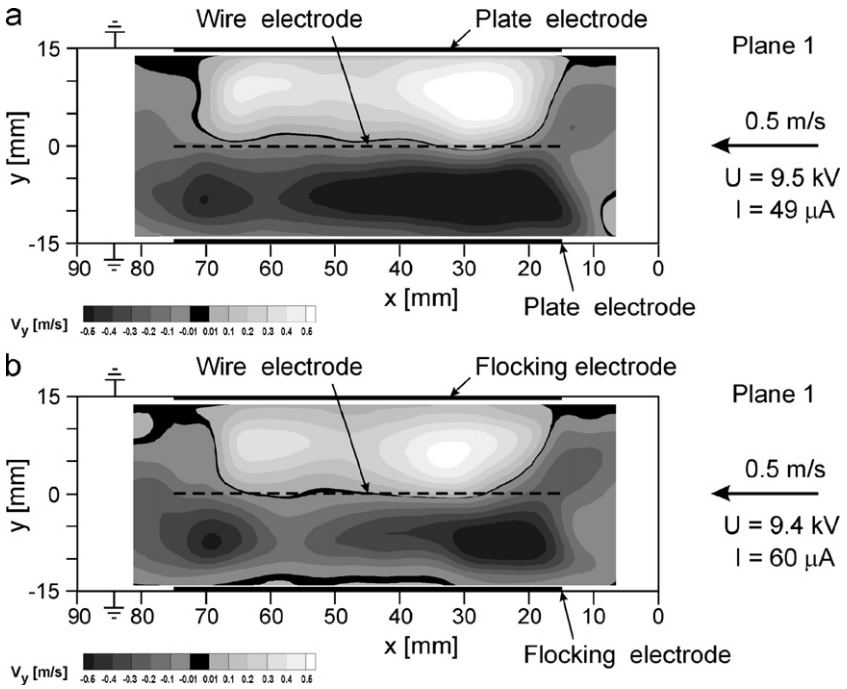

Fig. 7. Velocity y-component in plane 1: (a) in the wire-smooth-plate ESP for positive voltage of 9.5 kV and (b) in the wire-flocking plane ESP for positive voltage of 9.4 kV.

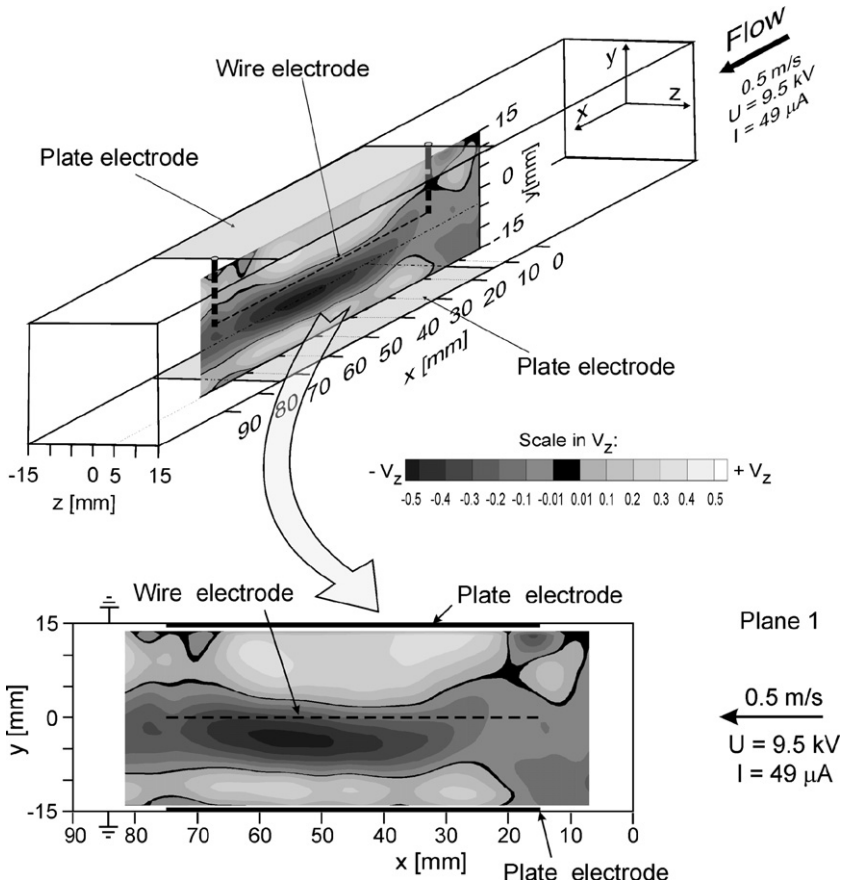

Fig. 8. Velocity z-component in plane 1 in the wire-smooth-plate ESP for positive voltage of 9.5 kV. Average discharge current 49 μA.

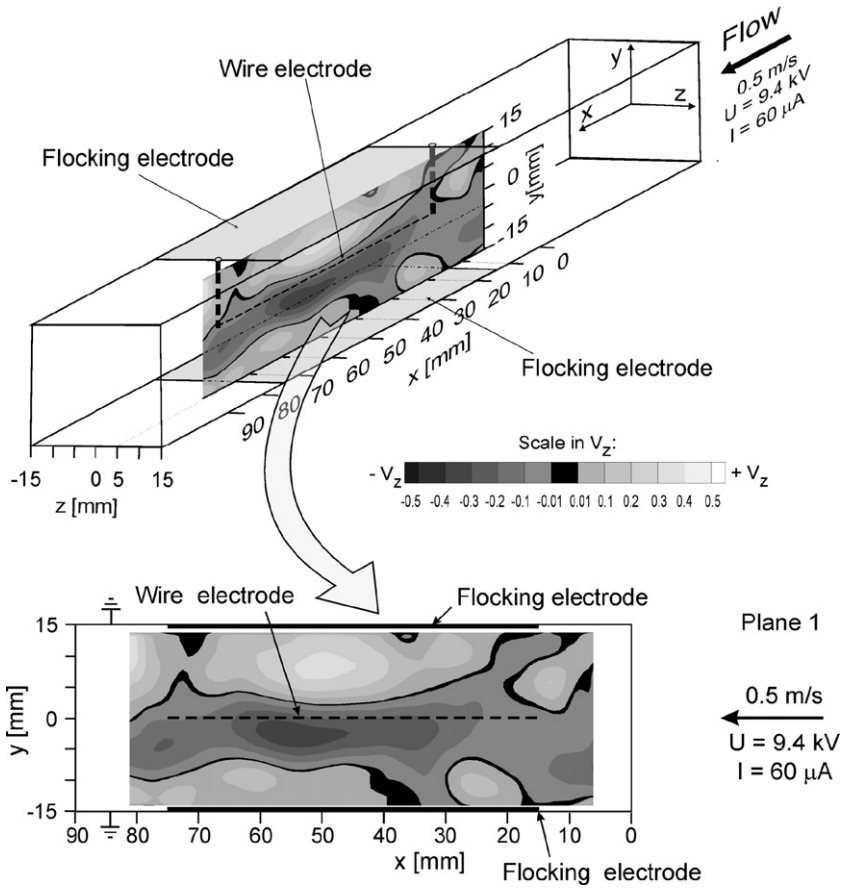

Fig. 9. Velocity z-component in plane 1 in the wire-flocking plane ESP for positive voltage of 9.4 kV. Average discharge current 60 μA.

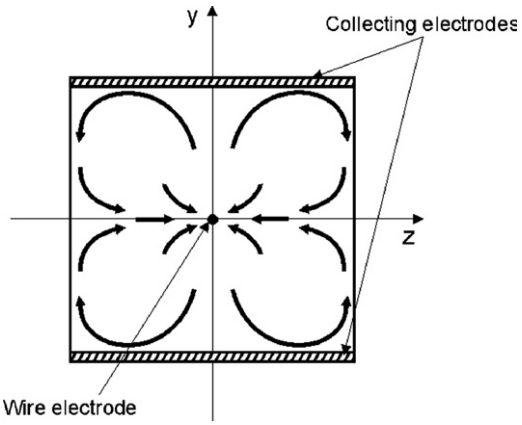

Fig. 10. Illustration of the anticipated transversal flow of the seed particles (y–z plane) in the narrow longitudinal ESP.

Similarly as in plane 1, the results obtained in plane 2 confirmed that the particle flow in both ESPs (the wire-smooth-plate and the wire-flocking plane ESP) had a 3D character caused by the applied voltage.

From the results presented in Figs. 4–9, one can deduce that in a narrow ESP with the wire discharge electrode placed longitudinal-to-flow the particles flow from the ESP center (near the discharge wire electrode) towards the collecting electrodes. Then, near the collecting electrodes the particles turn towards the side walls, and moved along them. In the middle part of the side walls the particles turn again towards the wire electrode. The suggested particle movement in a plane across the ESP duct (the plane y–z) in the central part of the discharge region is schematically shown in Fig. 10. Taking into account the strong longitudinal movement of the particles, one may imagine that the flow in the narrow longitudinal ESP has the form of four spiral vortices moving along the flow duct (in the x-direction).

4. Conclusions

The results of 3D PIV measurements of the particle velocity field in the narrow longitudinal ESP having either the wire-smooth-plate or wire-flocking plane electrode arrangements showed that the applied voltage significantly changed the particle flow pattern. When no voltage was applied the particle flow was laminar, whereas the applied voltage generated the secondary EHD flow which had a 3D character.

Comparing the results for the wire-smooth-plate ESP with those for the wire-flocking plane ESP, one can find that the movements of seed particles towards the collecting electrodes are very similar in both ESPs. However, in the case of the flocking plane electrodes the particle flow slows down in the vicinity of the collecting electrodes. This is

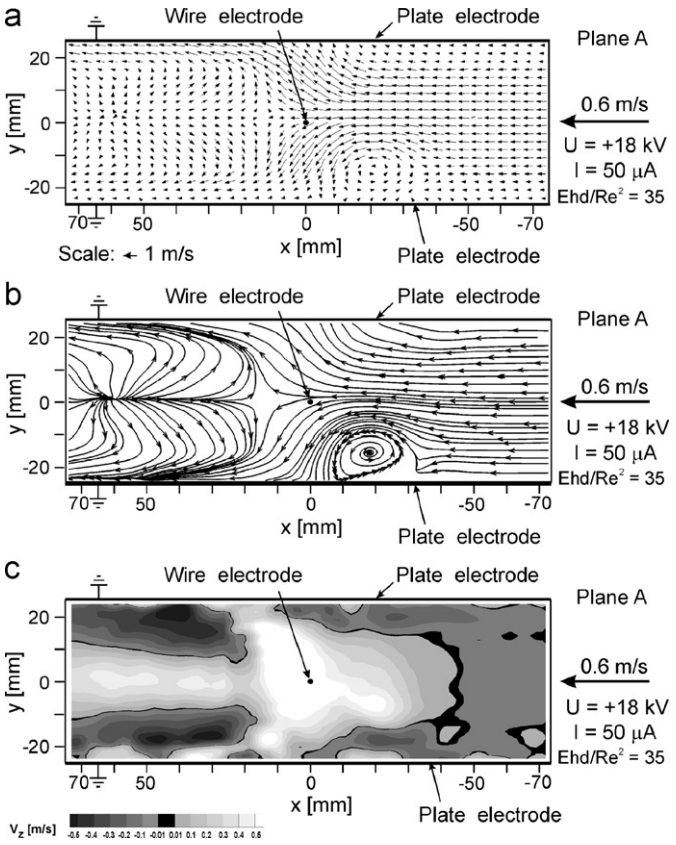

Fig. 11. Results of 3D PIV measurement (x–y plane) in the transverse wire-smooth-plate ESP for positive voltage of 18 kV [9]: (a) flow velocity field, (b) corresponding flow streamlines, and (c) velocity z-component. Average discharge current 50 μA. Plane A was set along the ESP in its center.

a quite beneficial effect because the slower flow near the collecting electrodes results in a smaller re-entrainment of the fine particles deposited on the collecting electrodes.

Furthermore, in the ESP with the wire electrode placed longitudinally to the flow duct the spiral vortices occur. They move along the ESP and do not block the primary flow, as it was observed in the ESPs with the wire electrode placed perpendicularly to the primary flow [6–10] (an example result is also shown in Fig. 11). This suggests that in the ESPs with the longitudinal-to-flow wire electrode, the pressure drop is lower and the flow along the ESP is smoother than in the ESPs with the wire electrode placed perpendicularly to the flow duct.

References

[1] A. Mizuno, Electrostatic precipitation, IEEE Trans. Dielectr. Electr. Insul. 7 (2000) 615–624.
[2] U. Kogelschatz, W. Egli, E.A. Gerteisen, Advanced computational tools for electrostatic precipitators, ABB Rev. 4 (1999) 33–42.
[3] B.J. Sung, A. Aly, S.H. Lee, K. Takashima, S. Katsura, A. Mizuno, Fine particles collection using an ESP equipped with electrostatic flocking filter as a collecting electrode, Plasma Process Polym. 3 (9) (2006) 661–667.
[4] A. Yabe, Y. Mori, K. Hijikata, EHD study of the corona wind between wire and plate electrodes, AIAA J. 16 (1978) 340–345.
[5] T. Yamamoto, H.R. Velkoff, Electrodynamics in an electrostatic precipitator, J. Fluid Mech. 108 (1981) 1–18.
[6] J. Mizeraczyk, M. Kocik, J. Dekowski, M. Dors, J. Podliński, T. Ohkubo, S. Kanazawa T. Kawasaki, Measurements of the velocity field of the flue gas flow in an electrostatic precipitator model using PIV method, J. Electrostat. 51–52 (2001) 272–277.
[7] J. Mizeraczyk, J. Dekowski, J. Podliński, M. Kocik, T. Ohkubo, S. Kanazawa, Laser flow visualization and velocity fields by particle image velocimetry in electrostatic precipitator model, J. Visualization 6 (2) (2003) 125–133.
[8] J. Mizeraczyk, M. Kocik, J. Dekowski, J. Podliński, T. Ohkubo, S. Kanazawa, Visualization and particle image velocimetry measurements of electrically generated coherent structures in an electrostatic precipitator model, Inst. Phys., Conf. Ser. 178 (2003) 167–173.
[9] J. Mizeraczyk, J. Podliński, M. Kocik, R. Barbucha, J.S. Chang, A. Mizuno, Experimental results on electrohydrodynamic flow in electrostatic precipitators, in: Fourth Asia-Pacific International Symposium on the Basic and Application of Plasma Technology, Cebu Workshop, Cebu, Philippines, 2005, pp. 29–33.
[10] J. Podliński, J. Dekowski, J. Mizeraczyk, D. Brocilo, J.S. Chang, Electrohydrodynamic gas flow in a positive polarity wire-plate electrostatic precipitator and the related dust particle collection efficiency, J. Electrostat. 64 (2006) 259–262.
[11] P. Atten, F.M.J. McCluskey, A.C. Lahjomri, The electrohydrodynamic origin of turbulence in electrostatic precipitators, IEEE Trans. Ind. Appl. 23 (1987) 705–711.
[12] T. Yamamoto, Effects of turbulence and electrohydrodynamics on the performance of electrostatic precipitators, J. Electrostat. 22 (1989) 11–22.
[13] A. Aly, B.J. Sung, S.H. Lee, A. Mizuno, The effect of different configurations of collecting electrodes on the flow visualization inside a wire-plate electrostatic precipitator (ESP) in the collecting electrodes, in: Annual Meeting of the Institute of Electrostatics, Japan, 2005.
[14] J. Westerweel, Fundamentals of Digital PIV, Meas. Sci. Technol. 8 (1997) 1379–1392.
[15] M. Raffel, Ch.E. Willert, J. Kompenhans, Particle Image Velocimetry. A Practical Guide, Springer, Berlin Heidelberg, 1998.
[16] IEEE-DEIS-EHD, Technical committee, recommended international standard for dimensionless parameters used in electrohydrodynamics, IEEE Trans. Dielectr. Electr. Insul. 10 (2003) 3–6.